Monatshefte für Chemie 136, 855–879 (2005)
DOI 10.1007/s00706-005-0297-8

Monatshefte für Chemie
Chemical Monthly
Printed in Austria

Invited Review

The Topological Analysis of the Electron Localization Function. A Key for a Position Space Representation of Chemical Bonds

Bernard Silvi[1,*], **Isabelle Fourré**[1], and **Mohammad E. Alikhani**[2]

[1] Laboratoire de Chimie Théorique (UMR 7616), Université Pierre et Marie Curie, Paris (France)
[2] Laboratoire de Dynamique, Interactions et Réactivité (UMR 7075), Université Pierre et Marie Curie, 75252-Paris cedex, France

Received October 12, 2004; accepted October 27, 2004
Published online April 4, 2005

Summary. The purpose of the topological theory of Chemical Bonding is to provide a mathematical bridge between chemical concepts, such as bonds and lone pair, and rigorous Quantum Mechanics. The theory of dynamical systems enables to achieve a partition of the geometrical molecular space into basins of attractors bearing a chemical significance. A one to one correspondence is established between these basins and the chemical objects used to describe the bonding. The definition of population operators gives access to quantitative information and provides a firm basis for the concept of mesomery.

Keywords. Bonding; Electronic structure; Localization function; Topological analysis.

Introduction

The celebrated mathematician and philosopher of Sciences *René Thom* said that he was not interested by Chemistry because concepts such as those of bond, valence, lack of scientific content [1]. By this statement he pointed out that the description of the matter at the microscopic level made by Chemistry was not as satisfactory as claimed by the community. Many of the related concepts are very difficult to define, for example the definitions of the chemical bond proposed by *Lewis* [2] (''two electrons thus coupled together, when lying between two atomic centers, and held jointly in the shells of two atoms, I have considered to be the chemical bond'') or by *Pauling* (''there is a chemical bond between two atoms or groups of atoms in case that the forces acting between them are such as to lead to the formation of an

* Corresponding author. E-mail: silvi@lct.jussieu.fr

aggregate with sufficient stability to make it convenient for the chemist to consider it as an independent molecular species'') [3] rely on beliefs rather than directly on facts.

In spite of its epistemological weaknesses, the concept of chemical bond derived from *Lewis*'s rule of two is essential in Chemistry because it provides a simple, efficient and robust tool enabling to predict as well as to explain the stoichiometry and the structure of almost all chemical systems in the ground state. The *Lewis*'s approach complemented by the VSEPR model [4–9] plays a very important role in Chemical Education. It is worth noting that the success of the valence and VSEPR models do not rely at all upon any underlying mathematical theory and indeed it seems to invalidate any reductionist attempt to derive Chemistry from Quantum Mechanics since the chemical bond is not a physical observable and therefore has no counterpart in Quantum Mechanics. As pointed out by *Malrieu* and *Maynau "La Chimie est moins une science de la régularité qu'une science des spécificités et de leur combinatoire, une science de la différence, de cette petite différence qui sépare un composé d'un composé faiblement substitué, ou d'un isomère."*[a] [10]. In other words, Chemistry has its own concepts, its own level of understanding which explains the properties of the matter from its composition in terms of elements and of their position in the periodic table rather than from physical laws mastered by the *Schrödinger* equation. Though we are conscious of the dangers of the temptation of reductionism, which at the end leads to throw away without further ado essential ''prequantum'' concepts of Chemistry such that of mesomery (according to *W. Kutzelnigg* [11]: ''The ''theory of mesomerism'' survived for a while because it was regarded as a mapping to simplified quantum chemical model, that of the semi-empirical valence-bond theory, until both the former and the latter became obsolete''), it is one of our tasks as theoretical chemists to build (when it is possible) a rigorous bridge between Chemistry and Quantum Mechanics.

A possible route to reach this goal has been proposed by *Dirac* in the last sentence of his 1929 paper ''Quantum Mechanics of Many-Electron Systems'' [12]: ''It therefore becomes desirable that approximate practical methods of applying quantum mechanics should be developed, which can lead to an explanation of the main features of complex atomic systems without too much computation.'' This prescription has been anticipated two years before *Dirac*'s paper by *Heitler* and *London* [13] on the one hand and by *Condon* [14] on the other hand. *Heitler* and *London*'s paper was immediately recognized as a milestone in the history of chemistry. Here was found the mathematical dynamic formulation of *Lewis'* covalent bond, the energy of the electron pair bond being given as a resonance energy due to the interchange of two electrons. As pointed out by *Pauling* [15]: ''*Condon*'s treatment is the prototype of the molecular-orbital treatment that has been extensively applied in the discussion of aromatic and conjugated molecules, and *Heitler* and *London*'s treatment is the prototype of the valence-bond method.'' These two methods constitute the backbone of the theory of chemical bonding. In the abstract of a recent paper *Hoffmann*, *Shaik*, and *Hiberty* write [16] ''Quantum Mechanics

[a] Chemistry is less a science of regularity than a science of specificities, of this small difference which distinguish a chemical compound from another weakly substituted or from an isomer

has provided Chemistry with two general theories, valence bond (VB) and molecular orbital (MO) theory. The two theories were developed at about the same time, but quickly diverged into rival schools that have competed, sometimes fervently, on charting the mental map and epistemology of chemistry." These methods have proved their efficiency in both predictive and interpretative purposes. However, the interpretative toolbox mostly relies on the interpretation of the approximate wave function in terms of its atom related components rather than upon observable quantities. For example, the orbital representation implies an arbitrary choice because orbitals are not invariant with respect to unitary transformations and the relationships with chemical concepts are therefore not always obvious, all the more so that orbitals are often considered in the vocabulary as real physical objects. As pointed out by *Coulson* [17]: "This epistemological difficulty is mostly due to the weakness of interpretative methods that give a physical significance to quantities, such as molecular orbitals or valence bond structures, appearing as intermediates during the course of solution of the many-body *Schrödinger* equation."

With the exception of seldom explicitly correlated wave functions such as that of *James* and *Coolidge* for dihydrogen [18], the VB and MO techniques have been for decades the unique methods enabling electronic calculations of many electron systems. Incidentally, we remark that the *James* and *Coolidge* wave function has not given rise to any class of interpretative methods. With the advent of the Density Functional Theory in 1964 [19], a third predictive method grown in importance, in a first step in Physics and in a further step in Chemistry (as soon as it was implemented in the *Gaussian* softwares [20]). With respect to the understanding of the bonding and of the reactivity of molecules, the Density Functional Theory has enabled to improve the scientific content of many concepts used by chemists (for a review see the review article of *Geerlings et al*. [21] and references herein). The first *Hohenberg-Kohn* theorem [19] states that a given ground state electron density distribution $\rho(\mathbf{r})$ corresponds to a unique number of electrons N and external potential (*i.e.* distribution of nuclei) which contains the whole chemical information. Moreover, according to the second *Hohenberg-Kohn* theorem the energy and the electron density can be directly obtained by solving the *Euler-Lagrange* equation of DFT and in principle the calculation of the wave function may be skipped as well as orbital expansions. Another attractive technique, the Quantum Monte Carlo method, has emerged during the thirty last years (for a comprehensive presentation of QMC applied to Chemistry see the book of *Hammond* and *Lester* [22]). Most of the interpretative techniques issued of the VB and MO approaches cannot be imported in the Monte Carlo framework because they rely on atomic basis functions.

In order to overcome these difficulties and to dispose of a general method of interpretation, it is necessary to build up a mathematical model of the chemical description of the matter, which is consistent with the postulates of Quantum Mechanics, valid for exact wave functions and therefore independent of the way of calculation of this latter or of an approximate one. This mathematical model is not unique because different spaces (geometrical direct space, momentum space, *Hilbert* space) as well as different mathematical theories external to Quantum Mechanics can be used for this purpose. The representation of the bonding in the geometrical space presents many advantages because chemists as more than

99.99% of human beings including crystallographers usually think in it. Recovery of the *Lewis*'s ideas from Quantum Mechanics in the geometrical space requires the help of an external mathematical theory enabling the analysis of a local function derived from density distributions and carrying the chemical information. The Loges theory of *Daudel* [23–27] make use of *Shannon*'s information theory [28] in order to find the best partition in adjacent regions which minimizes the missing information or the *a priori* indetermination. Unfortunately, the loge partitioning is hampered by its numerical complexity since its requires the evaluation of the *N*-particle density distribution and therefore its applications have been limited to very few systems. The dynamical system theory [29, 30] is another well established mathematical theory enabling the partition of space in adjacent volumes. Its advantage is that it is applied to the gradient vector field of a local function of the only variable **r**, the so-called potential function which contains the relevant chemical or physical information. The gradient dynamical system analysis has been introduced in Chemical Physics by *Richard Bader* [31] in the framework of the Atoms in Molecules (AIM) theory. *Bader* has shown that the gradient vector field of the one electron density distribution function enables to partition the space occupied by a molecule in atomic basins limited by zero-flux surfaces who enjoy the property of being quantum open system. The AIM theory recovers the chemical picture of the molecule made of atoms but the partition does not explicitly reveal a substructure corresponding to the cores and the valence shell of the atoms. The ELF [32] approach [33, 34] belongs to the same type of methodology, it attempts to overcome the conceptual limits of the topological analysis of the sole electron density. This method has been applied to study the bonding in molecules, complexes, and solids as well as reaction mechanisms.

The present paper intends to provide a pedagogical presentation of the method with a particular emphasis on its relations with the *Lewis*'s model.

The *Lewis*'s Model and Quantum Mechanics

Lewis imagined the cubic model of the atom in 1902. In this model an atomic kernel bearing a positive charge is surrounded by $n \leq 8$ static electrons occupying *n* vertexes of a cube. In the 1916 article [35], he uses the cubic atoms as parts of the molecular building set and the rules of the game are given by six postulates:

1. ''In every atom is an essential *kernel* which remains unaltered in all ordinary chemical changes and which possesses an excess of positive charges corresponding in number to the ordinal number of the group in the periodic table to which the element belongs.
2. The atom is composed of the kernel and an *outer atom* or *shell*, which, in the case of the neutral atom, contains negative electrons equal in number to the excess of positive charges of the kernel, but the number of electrons in the shell may vary during chemical change between 0 and 8.
3. The atom tends to hold an even number of electrons in the shell, and especially to hold eight electrons which are normally arranged symmetrically at the eight corners of a cube.

4. Two atomic shells are mutually interpenetrable.
5. Electrons may ordinarily pass with readiness from one position in the outer shell to another. Nevertheless they are held in position by more or less rigid constraints, and these positions and the magnitude of the constraints are determined by the nature of the atom and of such other atoms as are combined with it.
6. Electric forces between particles which are very close together do not obey the simple law of inverse squares which holds at greater distances.''

Though Quantum Mechanics enables to reject the idea of static electrons, a modern translation of the five first *Lewis*'s postulates (the role of the sixth postulate is to explain the uncomfortable idea of static electrons) can be given by an *ad hoc* partition of the geometrical position space in adjacent non overlapping volumes called hereafter *basins* in the following way:

1. The space occupied by an atom (with $Z>2$) is divided into an inner region the *core basin* encompassing the nucleus and an external region, the atomic valence shell, gathering its *valence basins* which may extend to infinity.
2. A valence basin may be shared by the valence shells of several atoms.
3. There is a high probability to find $Z-n_v$ electrons within a core basin where n_v is the ordinal number of the group of the periodic table to which the element belongs (in other words the conventional number of valence electrons).
4. There is a high probability to find an even number of electrons in a valence basin belonging to a closed shell system.

The validity of these propositions relies on the one hand upon our ability to carry out the electron count for an arbitrary partition and on the other hand on the availability of a reliable partitioning technique.

The Basin Population Operator

The electron count over a basin, say Ω_A, is performed with the help of the population operator introduced by *Diner* and *Claverie* [36] (Eq. (1)) where N denotes the total number of electrons. The population operator of the union of two basins Ω_A and Ω_B is given by Eq. (2) which is not the sum $\hat{N}(\Omega_A)+\hat{N}(\Omega_B)$. Considering the whole space, *i.e.* $\bigcup_A \Omega_A$ one gets the sum rule (Eq. (3)).

$$\hat{N}(\Omega_A)=\sum_i^N \hat{y}(\mathbf{r}_i) \quad \text{with } \hat{y}(\mathbf{r}_i)\begin{cases}\hat{y}(\mathbf{r}_i)=1 & \mathbf{r}_i\in\Omega_A\\ \hat{y}(\mathbf{r}_i)=0 & \mathbf{r}_i\notin\Omega_A\end{cases} \tag{1}$$

$$\hat{N}(\Omega_A\cup\Omega_B)=\sum_i^N \hat{y}(\mathbf{r}_i) \quad \text{with } \hat{y}(\mathbf{r}_i)\begin{cases}\hat{y}(\mathbf{r}_i)=1 & \mathbf{r}_i\in\Omega_A\cup\Omega_B\\ \hat{y}(\mathbf{r}_i)=0 & \mathbf{r}_i\notin\Omega_A\cup\Omega_B\end{cases} \tag{2}$$

$$\hat{N}\left(\bigcup_A \Omega_A\right)=N \tag{3}$$

The eigenvalues, $N(\Omega_A)$, of $\hat{N}(\Omega_A)$ belong to the series of integer $0, \ldots, N$ and represent all the accessible numbers of electrons within Ω_A. As a consequence of Eq. (3), the eigenvalues of the population operators of different basins are correlated since they also obey the closure relation (Eq. (4)).

$$\sum_A N(\Omega_A) = N \tag{4}$$

The expectation values of the population operators, $\bar{N}(\Omega_A)$ (Eq. (5)), can be expressed in terms of the volume integral of the one electron probability distribution over the basins. They are real numbers and can be understood as the average of the measurements of the electron numbers $N(\Omega_A)$. They also fulfill a closure relation, *i.e.* Eq. (6).

$$\bar{N}(\Omega_A) = \langle \Psi | \hat{N}(\Omega_A) | \Psi \rangle = \int_{\Omega_A} \rho(\mathbf{r}) d\mathbf{r} \tag{5}$$

$$\sum_A \bar{N}(\Omega_A) = N \tag{6}$$

In fact, these eigenvalues and expectation values are determined simultaneously. Each set of eigenvalues defines an accessible chemical electronic structure and the expectation values $\bar{N}(\Omega_A)$ can be therefore interpreted as weighted averages of resonance structures.

The closure relation of the basin population operators enables to carry out a statistical analysis of the basins populations through the definition of a covariance matrix [37]. The covariance operator is a matrix operator whose elements are deduced from the classical expression of the covariance (Eq. (7)).

$$\widehat{cov}(\Omega_A, \Omega_B) = \hat{N}(\Omega_A)\hat{N}(\Omega_B) - \bar{N}(\Omega_A)\bar{N}(\Omega_B) \tag{7}$$

The covariance matrix element expectation values are the difference between the actual pair populations $\bar{\Pi}(\Omega_A, \Omega_B)$ and their "classical" analogs $\bar{N}(\Omega_A)\bar{N}(\Omega_B)$ or $\bar{N}(\Omega_A)(\bar{N}(\Omega_A) - 1)$ in the case of the diagonal elements given by Eq. (8).

$$\begin{aligned} \langle \widehat{cov}(\Omega_A, \Omega_A) \rangle &= \bar{\Pi}(\Omega_A, \Omega_A) - \bar{N}(\Omega_A)(\bar{N}(\Omega_A) - 1) \\ \langle \widehat{cov}(\Omega_A, \Omega_B) \rangle &= \bar{\Pi}(\Omega_A, \Omega_B) - \bar{N}(\Omega_A)\bar{N}(\Omega_B) \end{aligned} \tag{8}$$

The diagonal elements of the covariance matrix (the variances), are often noted $\sigma^2(\bar{N})$ as they classically represent the square of the standard deviation σ.

In the case of open shell systems it is also very interesting to localize the unpaired electron by calculating the integrated spin density over localization basins.

Although, the topological representation proposes a rather satisfactory interpretation of the bonding, reliable descriptions in terms of superposition of chemical structures are often very helpful, at least, as explanatory models. As it has been proposed in two previous papers [37, 38], the data provided by the topological analysis can be used to build such models and also to discuss their ability to describe the distribution of the electrons.

Table 1. Core radius r_c (a.u.), core populations $\bar{N}_c$, and variance of core populations $\sigma^2(\bar{N}_c)$ calculated from the variance minimization and ELF

	Variance minimization			ELF		
	r_c	$\bar{N}_c$	$\sigma^2(\bar{N}_c)$	r_c	$\bar{N}_c$	$\sigma^2(\bar{N}_c)$
Li	1.573	2.011	0.065	1.610	2.019	0.066
Be	0.998	2.009	0.103	1.015	2.018	0.103
B	0.716	2.015	0.155	0.688	1.986	0.157
C	0.550	2.017	0.206	0.586	2.073	0.211
N	0.433	2.007	0.265	0.472	2.100	0.275
O	0.358	1.996	0.308	0.410	2.166	0.334
F	0.302	1.977	0.348	0.364	2.240	0.400
Ne	0.259	1.953	0.383	0.295	2.151	0.408
Na	2.310	10.071	0.167	2.261	10.053	0.167
Mg	1.711	10.075	0.283	1.662	10.032	0.285
Al	1.412	10.074	0.337	1.426	10.092	0.337
Si	1.194	10.067	0.397	1.155	9.993	0.402
P	1.030	10.057	0.457	1.027	10.050	0.458
S	0.907	10.051	0.506	0.878	9.957	0.512
Cl	0.809	10.046	0.554	0.800	10.010	0.554
Ar	0.730	10.044	0.598	0.736	10.070	0.598
K	3.365	18.139	0.214	3.293	18.114	0.214
Ca	2.595	18.155	0.382	2.491	18.065	0.387
Ga				1.581	27.820	0.888
Ge	1.643	28.509	0.874	1.371	27.673	1.004
As	1.413	28.340	0.980	1.278	27.812	1.041
Se	1.269	28.277	1.065	1.143	27.663	1.147
Br	1.157	28.264	1.108	1.119	28.051	1.118
Kr	1.064	28.187	1.217	1.012	27.838	1.244

The Topological Partition

To be faithful to the *Lewis*'s picture, the partition we are considering should yield electron counts in the core and valence basins in agreement with prescriptions made above: the population of the core basins should be close to $Z - n_v$ and its variance should be small, that of valence basins should be either close to an even number with a small variance or to an odd number with a variance of the order of 1. Table 1 reports the core radii (r_c), the core populations ($\bar{N}_c$), and their variance ($\sigma^2(\bar{N}_c)$) of the 2nd, 3rd, and 4th periods main group elements calculated by variance minimization as well as from ELF. For all atoms, except gallium, both the variance minimization and ELF yield core populations close to the expectations. As an example one can consider the Mg atom for which Fig. 1 displays the variance of $\bar{N}(R)$, the integrated density in a sphere of radius R centered on the nucleus, as a function of $\bar{N}(R)$. The two minima are found for $\bar{N}(R) \simeq 2$ and $\bar{N}(R) \simeq 10$ which correspond to the occupancy of the K and $K + L$ shells.

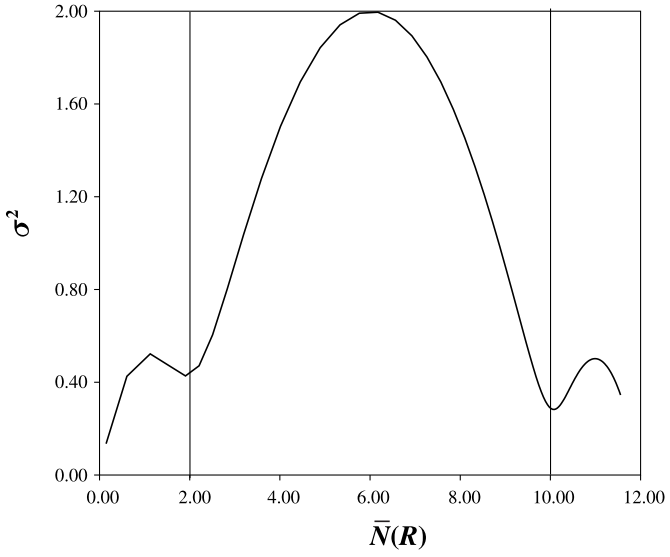

Fig. 1. σ^2 *vs.* $\bar{N}(R)$ for Mg

The minimization of the variance with respect to the core volume implies that the variational equation (Eq. (9)) should be satisfied. This equation can be written in terms of a surface integral (Eq. (10)) in which $\eta(\mathbf{r})$ is a scalar function for which the bounding surface S is a zero flux surface. In the theory of dynamical systems [29, 30], a volume limited by such a surface is the basin of an attractor of the gradient vector field of the *potential function* $\eta(\mathbf{r})$.

$$\frac{\delta\sigma^2(\bar{N})}{\delta V} = 0 \tag{9}$$

$$\frac{\delta\sigma^2(\bar{N})}{\delta V} = \oint_S \mathbf{n} \cdot \nabla\eta(\mathbf{r}) ds = 0 \tag{10}$$

In principle the $\eta(\mathbf{r})$ function can be evaluated from the expression of $\sigma^2(\bar{N})$, however it is more efficient to use an analytical function such as ELF able to do the same job.

The ELF Function

The electron localization function ELF [32] is basically the ratio of the *Laplac*ian of the conditional probability $D(\mathbf{r}) = \nabla^2_{\mathbf{r}} P^{\sigma\sigma}_{\text{cond}}(\mathbf{r}, \mathbf{r}')|_{\mathbf{r}'=\mathbf{r}}$ by the electron density raised at the power $5/3$, $D_0(\mathbf{r})$. Different physical interpretations have been proposed of the ELF formula in order to justify the denominator. *Savin et al.* [39–41] have remarked that the *Laplac*ian of the conditional probability is the difference of the definite positive kinetic energy densities of the actual system and of an equivalent density model system in which the antisymmetry is switched off, that is the excess kinetic energy due to the *Pauli* principle whereas the denominator is the

same quantity calculated for homogeneous electron gas reference. The *Lorentz*ian form (Eq. (11)) enables to confine the ELF values in the $[1, 0]$ interval. The function tends to 1 where parallel spins are highly improbable (mostly regions dominated by a single opposite spin pair) and to zero in regions where there is a high probability of same spin pairs.

$$\eta(\mathbf{r}) = \frac{1}{1 + \left(\frac{D(\mathbf{r})}{D_0(\mathbf{r})}\right)^2} \tag{11}$$

Another local descriptor of the pair formation in the sense of *Lewis*'s model, the so-called spin pair composition, has recently been introduced on the basis of the two particle probability density analysis [42]. This function is defined as the ratio of same spin and opposite spin pair functions integrated over a sampling volume around the reference point (Eq. (12) with Eq. (13)).

$$c_\pi(\mathbf{r}) = \bar{N}(\mathbf{r})^{-2/3} \frac{\bar{N}_\parallel(\mathbf{r})}{\bar{N}_\perp(\mathbf{r})} \tag{12}$$

$$\begin{aligned} \bar{N}(\mathbf{r}) &= \int_V \rho(\mathbf{r}_1) d\mathbf{r}_1 \\ \bar{N}_\parallel(\mathbf{r}) &= \int_V \int_V \pi^{\alpha\alpha}(\mathbf{r}_1, \mathbf{r}_2) d\mathbf{r}_1 d\mathbf{r}_2 + \int_V \int_V \pi^{\beta\beta}(\mathbf{r}_1, \mathbf{r}_2) d\mathbf{r}_1 d\mathbf{r}_2 \\ \bar{N}_\perp(\mathbf{r}) &= \int_V \int_V \pi^{\alpha\beta}(\mathbf{r}_1, \mathbf{r}_2) d\mathbf{r}_1 d\mathbf{r}_2 + \int_V \int_V \pi^{\beta\alpha}(\mathbf{r}_1, \mathbf{r}_2) d\mathbf{r}_1 d\mathbf{r}_2 \end{aligned} \tag{13}$$

In these equations $\rho(\mathbf{r})$ is the spinless one electron density distribution function, and $\pi^{\sigma\sigma'}(\mathbf{r}_1, \mathbf{r}_2)$ the $\sigma\sigma'$ component of the two particle distribution $\pi(\mathbf{r}_1, \mathbf{r}_2)$. It has been shown that ELF is an excellent approximation to this function once put in the *Lorentz*ian form $\eta(\mathbf{r}) = (1 + c_\pi^2(\mathbf{r}))^{-1}$. ELF has the advantage that it can be expressed analytically in terms of basis functions in all practical cases where the wave function is expressed in terms of orbitals, whereas the spin pair composition must be calculated numerically.

A Sketch of the ELF Analysis

As already mentioned, the gradient dynamical system theory appears to be the convenient mathematical tool to perform a partition of the space in regions dominated by a single electron pair or by a single (unpaired) electron. A glossary of the mathematical vocabulary used hereafter is given in Appendix A. The principles of the method are the following: consider a local function, say $\eta(\mathbf{r})$ called potential function in the dynamical system theory context, which carries the chemical information; its gradient $\nabla\eta(\mathbf{r})$ forms a vector field bounded on $\mathbb{R}^3$. The $\nabla\eta(\mathbf{r})$ field determines two types of points of $\mathbb{R}^3$, on the one hand the wandering points at which $\nabla\eta(\mathbf{r}_w) \neq 0$ and on the other hand the critical points which correspond to $\nabla\eta(\mathbf{r}_c) = 0$. Each critical point is characterized by its index I_P which is the number of positive eigenvalues of the second derivative (*Hess*ian) matrix of

$\eta(\mathbf{r})$. The number and type of critical points obeys the *Poincaré-Hopf* formula, *i.e.* Eq. (14) with $\chi(M)=1$ for a molecule and 0 for a periodic system. The potential function implicitly depends upon a set of parameters, called control space. The formal analogy with a velocity field (*i.e.* $\nabla\eta(\mathbf{r}) = d\mathbf{r}/dt$) enables to build trajectories by integrating over the time variable. Each trajectory starts in the neighborhood of a point (or set of points) for which $\nabla\eta(\mathbf{r}) = 0$ called the α-limit and ends in the neighborhood of another point (or set of points) for $\nabla\eta(\mathbf{r}) = 0$ called the ω-limit. Except for asymptotic behaviors, the α and ω-limits are critical points. The set of trajectories having a given critical point as ω-limit is called the stable manifold of this critical point whereas its unstable manifold is the set of trajectory for which it is a α-limit. The stable manifold of a critical point of index 0 (a local maximum or *attractor*) is the basin of the attractor, that of a critical point of index larger than 0 is a separatrix: it is the boundary between basins.

$$\sum_P (-1)^{I_P} = \chi(M) \tag{14}$$

The topological partition of the ELF gradient field [34, 43] yield basins of attractors which can be thought as corresponding to bonds and lone pairs. As the ELF function is totally symmetrical the attractors can be single points (general case), circles (off axis attractors of linear molecules), or spheres (off center attractors of atoms) according to their location and to the molecular symmetry. In a molecule one can find two types of basins. On the one hand are core basins surrounding nuclei with atomic number $Z>2$ and labeled C(A) where A is the atomic symbol of the element and on the other hand are the valence basins. The valence basins are characterized by the number of atomic valence shells to which they participate, or in other words by the number of core basins with which they share a boundary. This number is called the synaptic order. Thus, there are monosynaptic, disynaptic, trisynaptic basins, and so on. Monosynaptic basins, labeled V(A), correspond to the lone pairs of the *Lewis* model, and polysynaptic basins to the shared pairs of the *Lewis* model. In particular, disynaptic basins, labeled V(A, X) correspond to two-centre bonds, trisynaptic basins, labeled V(A, X, Y) to three-centre bonds, and so on. The valence shell of a molecule is the union of its valence basins. As hydrogen nuclei are located within the valence shell they are counted as a formal core in the synaptic order because hydrogen atoms have a valence shell. For example, the valence basin accounting for a C–H bond is labeled V(C, H) and called protonated disynaptic. The valence shell of an atom, say A, in a molecule is the union of the valence basins whose label lists contain the element symbol A.

In the *Born-Oppenheimer* approximation, the wave function and, therefore, the electron localization function parametrically depend upon the set of nuclear coordinates which forms the control space. *Thom*'s catastrophe theory [1] provides a convenient mathematical model for the study of the bonding evolution with respect to changes of the control space parameters [44]. Within the framework provided by the ELF analysis, a chemical reaction is viewed as a series of topological changes occurring along the reaction path. The parameters defining

the reaction pathway (such as the nuclear coordinates and the electronic state) constitute the control space. The evolution of the bonding along the reaction path is modeled by the changes in the number and synaptic orders of the valence basins. Each structure is only possible for values of the control parameters belonging to definite ranges, in other words to subsets called structural stability domains. Along the reaction path the chemical systems goes from a structural stability domain to another by means of bifurcation catastrophes occurring at the turning points. Each catastrophe transforms the overall topology in such a way as the *Poincaré-Hopf* relation is fulfilled. This technique shows how the bonds are formed and broken and also emphasize the importance of the geometrical constraints in chemical reactions. For example, the breaking of a covalent bond is characterized by the increase of the number of basins through a cusp catastrophe which transforms the attractor of the V(A, B) disynaptic basin into a critical point of index one and the two attractors of the new monosynaptic basins V(A) and V(B).

The concept of localization domain has been introduced [45] for graphical purposes and also in order to define a hierarchy of the localization basins which can be related to chemical properties. A localization domain is a volume limited by one or more closed isosurfaces $\eta(\mathbf{r}) = f$. A localization domain surrounds at least one attractor, in this case it is called irreducible. If it contains more than one attractor it is reducible. Except for atoms and linear molecules, the irreducible domains are always filled volumes whereas the reducible ones can be either filled volumes, hollow volumes, or donuts. Upon the increase of the value of $\eta(\mathbf{r})$ defining the bounding isosurface, a reducible domain splits into several domains each containing less attractors than the parent domain. The reduction of localization occurs at turning points which are critical points of index 1 located on the separatrix of two basins involved in the parent domain. Ordering these turning points (localization nodes) by increasing $\eta(\mathbf{r})$ enables to build tree-diagrams reflecting the hierarchy of the basins [46]. A core basin is counted in the synaptic order of valence basins if there exist a value of the localization function which gives rise to an hollow volume localization domain (containing the considered valence basin attractors) with the core domain in its hole. Figure 2 displays the localization domains of methanol corresponding to isosurfaces defined by three values of $\eta(\mathbf{r})$. For $\eta(\mathbf{r}) < 0.1$, there is an unique parent domain encompassing all the attractors, the successive bifurcations occur at 0.11, 0.13, 0.53, 0.71, 0.805, and 0.905 as represented by the reduction of localization diagram in Fig. 3.

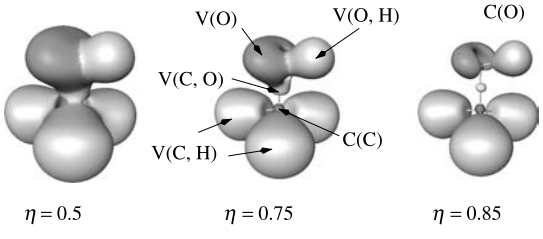

Fig. 2. $\eta(\mathbf{r}) = 0.5, 0.75$, and 0.85 localization domains of CH_3OH

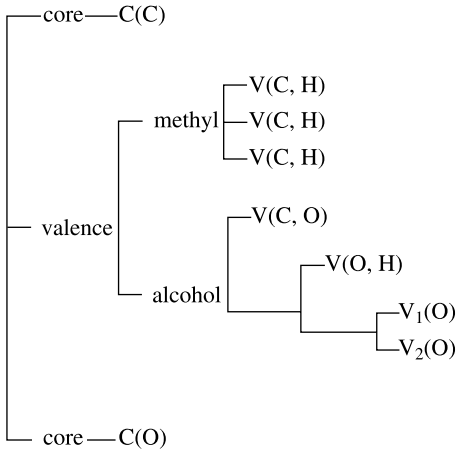

Fig. 3. Reduction of localization diagram of CH_3OH

Bonding Classification Criteria

The interactions between molecules have been classified by *R. Bader* into closed-shell and shared-electron interactions [31]. The closed-shell type includes interactions related with a chemical reaction such as ionic bonds as well as weaker interactions due to electrostatic or dispersion forces. The shared-electron interaction includes covalent, dative, and metallic bonding as subclasses. The criteria retained by *Bader* to discuss the type of bonding are on the one hand the occurrence of a bond path between two atomic attractors and on the other hand the sign of the *Laplac*ian of the density at the bond critical point [31]. In the AIM approach a bond path is defined as the unstable manifold (see Appendix A) of a critical point of index 1, the so-called bond critical point, which is a saddle point located at the boundary of two atomic basins. The bond path is formed by two trajectories linking this critical point to the attractors of the two atomic basins. A negative value of $\nabla^2\rho(r_c)$ is the signature of the shared interaction whereas a positive value indicates a closed shell interaction. The density of energy at the bond critical point has been further introduced by *Cremer* and *Kraka* [47, 48] in order to refine the discussion of the bonding. More recently, *Bianchi et al.* [49] have proposed a set of indicators enabling an assignment in terms of the different subclasses of the shared and closed-shell interactions. In addition to these rather qualitative criteria, quantitative information is provided by the atomic basin populations and by the related covariance analysis [50] interpreted in terms of ''topological bond orders'' [51, 52] or of delocalization indexes [53–55].

In the ELF gradient field analysis, the shared and unshared interactions are unambiguously identified by an unique topological criterion: the presence or the absence of a di- or polysynaptic basin [34, 45]. This argument is fully consistent with the *Lewis*'s picture since a polysynaptic basin is the common part of several atomic valence shells. As already discussed above, the quantitative analysis provides basin populations and related covariance matrices which can be exploited to reinterpret the bonding in terms of averaged mesomeric structures. The subclasses of both interactions are determined by studying the topological behaviour of the

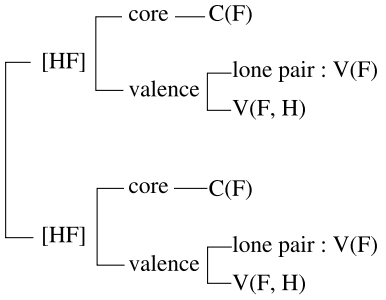

Fig. 4. Reduction of localization diagram of HF_2

gradient field along the dissociation reaction pathway [44]. For example, breaking a covalent bond increases the number of basins by one because the disynaptic basin encountered at equilibrium geometry is split into two monosynaptic ones. In the case of conventional multiple bonds, the bond multiplicity is not automatically correlated to an equal multiplicity of the disynaptic basins. On the one hand, the location of the attractors should be consistent with the point symmetry and therefore the disynaptic basins multiplicity can be explained by symmetry considerations rather than by chemical arguments. On the other hand, conventional multiple bonds are often limit resonance structures (for example $|C{\equiv}O|$) which are seldom the dominant ones. In a recent paper [56] *D. B. Chesnut* has discussed the bond multiplicity in the AIM and ELF framework and concluded that the measures are dependent on the nature of the *AB* pair.

Moreover, the ELF analysis provides topological arguments enabling to decide whether an interaction is chemical or not [44]. The gradient field of the potential function of a complex formed from neutral species at infinite separation is either the addition of those of its moieties or something different. In the former case where the number and the synaptic orders of the basins is the same at any distances less or equal to the equilibrium distance, the interaction is not the consequence of a chemical reaction and therefore it cannot be defined as chemical. This situation occurs for *van der Waals* and electrostatic interactions including weak and medium hydrogen bonds [57]. In the case of a chemical interaction at least the synaptic order of one basin changes. The use of reduction of localization diagrams is the convenient tool enabling to decide whether a system can be considered as a single chemical entity. For example, the reduction of localization diagram of the $(FH)_2$ complex displayed in Fig. 4 clearly shows that the first bifurcation splits the parent domain in two reducible domains corresponding to the two interacting hydrogen fluoride molecules.

The Electron Shared Interactions

The electron shared interaction includes the covalent, dative, and metallic bondings as subclasses. The presence of a di- or polysynaptic basin can be interpreted as arising from the dominant mesomeric structure and, with this respect, the quantitative analysis provides additional pieces of information on the delocalization and on weights of ionic contributions.

Covalent Bonds

The C–C bond of ethane is an archetype of covalent bond, the topology of the ELF gradient field of this molecule is represented in Fig. 5 for two representative values of the C–C internuclear distance, namely 3.0 Å and the equilibrium distance 1.53 Å. When the covalent bond is formed, the two monosynaptic basins represented in light grey merge into a single disynaptic one in grey. The interpretation in terms of catastrophe theory indicates that the bond formation (or dissociation) can be modeled by a cusp catastrophe [44].

Figure 6 displays the localization domains of four unsaturated hydrocarbons: ethylene, acetylene, allene, and benzene. The conventional double bond of ethylene gives rise to two disynaptic basins on both sides of the σ_h symmetry plane whereas for acetylene the axial symmetry yields a unique disynaptic basin the attractor of which is degenerated on a circle perpendicular to the C_∞ axis. In ethylene and in allene, the V(C, C) and V(C, H) are arranged in staggered position in order to minimize the *Pauli* repulsion between them in agreement with the VSEPR expectation. In benzene, there are six V(C, C) basins with a shape intermediate between those of a typical single bond (ethane, for example) and of a double bond. Conventional C=N double bonds, as in CH_2NH (Fig. 7), give rise to two basins whereas a single bean shaped disynaptic basin arises for the

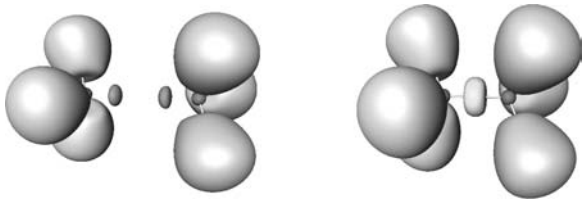

Fig. 5. $\eta(\mathbf{r}) = 0.8$ localization domains of C_2H_6; left R = 3.0 Å, right R = 1.530 Å

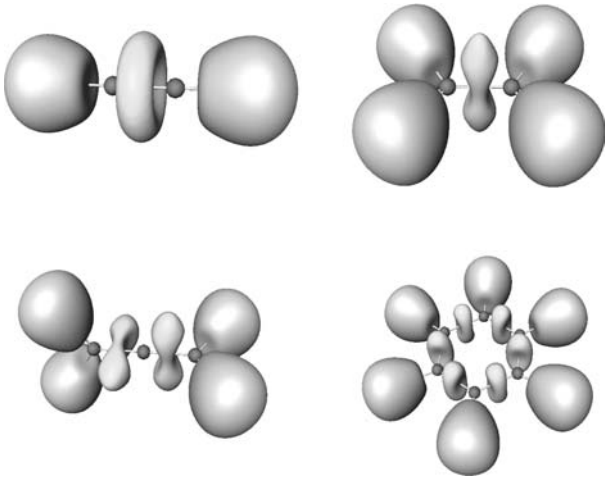

Fig. 6. $\eta(\mathbf{r}) = 0.8$ localization domains of C_2H_2 (top left), C_2H_4 (top right), C_3H_4 (bottom left), and C_6H_6 (bottom right)

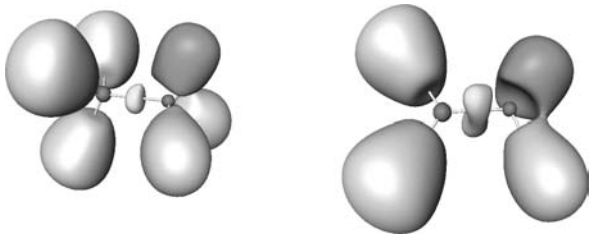

Fig. 7. $\eta(\mathbf{r}) = 0.8$ localization domains of CH_3NH_2 (left) and CH_2NH (right)

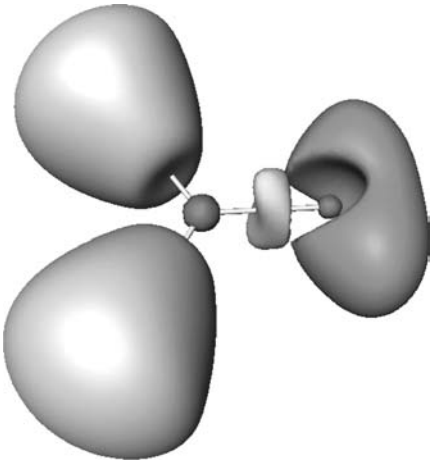

Fig. 8. $\eta(\mathbf{r}) = 0.8$ localization domains of CH_2O

Table 2. Basin populations ($\bar{N}$) and variance of basin populations (σ^2) of V(C, *X*), V(C, H), V(*X*, H) disynaptic and V(*X*) monosynaptic basins; (2) indicates the multiplicity of the basin, (*t*) a circular attractor

	V(C, *X*)		V(C, H)		V(*X*, H)		V(*X*)	
	$\bar{N}$	σ^2	$\bar{N}$	σ^2	$\bar{N}$	σ^2	$\bar{N}$	σ^2
C_2H_6	1.81	0.97	2.0	0.64				
C_2H_4	1.69(2)	0.95	2.11	0.64				
C_2H_2	5.14(*t*)	1.38	2.32	0.70				
C_3H_4	1.85(2)	0.99	2.08	0.67				
C_6H_6	2.76	1.30	2.15	0.66				
CH_3NH_2	1.62	0.94	2.02	0.64	1.96	0.77	2.17	0.97
CH_2NH	1.47(2)	0.90	2.13	0.63	1.95	0.74	2.64	1.07
HCN	4.30(*t*)	1.55	2.29	0.68			3.22	1.17
CH_3OH	1.24	0.80	2.04	0.63	1.70	0.79	2.36(2)	1.08
CH_2O	2.42	1.32	2.14	0.60			2.54(2)	1.12

isoelectronic CH_2O displayed in Fig. 8. These different features can be interpreted in the light of the population analysis reported in Table 2. On the one hand, the V(C, *X*) basin populations decrease as the electronegativity difference increases

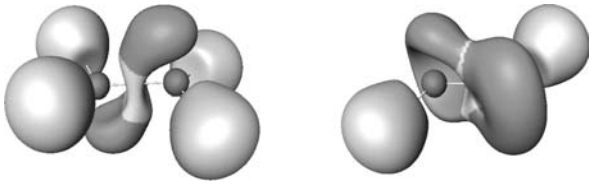

Fig. 9. $\eta(\mathbf{r}) = 0.8$ localization domains of Si_2H_4 (left) and Si_2H_2 (right)

which corresponds to a charge transfer towards both V(C, H) and V(X) basins. In terms of mesomery, as expected the weight of the ionic structure $C^{\oplus}$–$X^{\ominus}$ increases which is consistent with the behavior of the V(X) population and with *Sanderson*'s lone pair bond weakening effect whereas the $C^{\ominus}$–$X^{\oplus}$ accounts for that of V(C, H). The same trend is observed in the case of formal multiple CX bonds. On the other hand, for a given X, the increase of V(C, H) and V(X) basin populations with the bond multiplicity is achieved at the expend of the V(C, X) populations.

Classical multiple bonds mostly occur between elements belonging to the second period whereas elements of higher periods seems to prefer ''slipped bonds'' or multicenter bonds. In orbital related pictures, this behavior is explained by the hybridization defect [58]. *Grützmacher* and *Fässler* have shown that the ELF analysis enables to distinguish between slipped and unslipped bonds [59], for Si_2H_4 the lowest energy isomer has a trans bent structure involving such a slipped bond. The comparative study of the Si_2H_2 isomers carried out by *D. B. Chesnut* [60] concludes that the H-bridged structures are more stable than the trans bent one. Figure 9 displays the localization domains of the trans bent structures of Si_2H_4 and Si_2H_2. In Si_2H_4, the slipped double bond corresponds to two disynaptic basins V(Si, Si) with a population $\bar{N} = 0.85$ and two monosynaptic ones with $\bar{N} = 1.07$, the variances of these populations are rather large, 0.72 and 0.62 respectively, which are essentially accounted for by the covariance matrix elements between them. In Si_2H_2, there are four monosynaptic basins, each with a population of 1.23 and a monosynaptic one with only $\bar{N} = 0.99$. Again the covariance analysis shows a strong delocalization between these basins.

Dative Bonds

The BH_3NH_3 molecule is the archetype of the dative bond, Fig. 10 displays the localization domains for two B–N distances corresponding to a dissociated structure and the equilibrium geometry. When a dative bond is formed, the number of

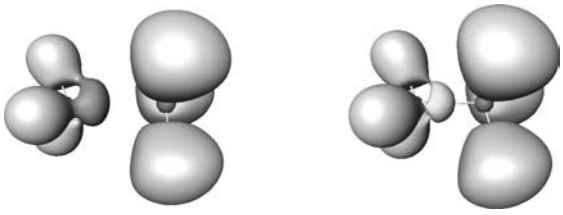

Fig. 10. $\eta(\mathbf{r}) = 0.8$ localization domains of BH_3NH_3, left $R_{BN} = 2.5$ Å and right $R_{BN} = 1.665$ Å

basins is conserved but a monosynaptic basin becomes disynaptic (for a detailed analysis see Ref. [44]. The formation of the B–N bond does not yield any charge transfer between the two moieties but a small one within the ammonia subunit from the V(B, N) basin towards the V(N, H) since the population of the former is 1.93 at $R_{BN} = 2.5$ Å against 1.88 at the equilibrium distance.

In transition metal carbonyls, the *M*–CO bonds are of the dative type but are characterized by a noticeable electronic transfer from the metal towards the CO groups. The ELF analysis carried out on the monocarbonyl complexes enabled *Pilmé et al*. [61] to draw the following conclusions: The formation of a *M*CO complex in which *M* is a transition metal atom of atomic number $Z = 20 + n$ obeys the following rules:

1. Except for $n = 4, 5, 9$, the spin multiplicity obeys *Hund*'s rule for the configuration $[\mathrm{Ar}]c^{n+2}$.
2. The averaged local configuration of the core is rather $[\mathrm{Ar}]c^{n}$ except for Cr and Cu for which it is $[\mathrm{Ar}]c^{n+1}$ as expected from the electronic configuration of the ground state of the free atom.
3. For $n<4$ the stable configuration multiplicity is $n + 3$. Since the local core configuration is mostly $[\mathrm{Ar}]c^{n}$, two unpaired electrons can be shared by the metal valence basin, the ligand, and the metal core. Therefore the total charge transfer and the V(*M*) population are both close to 1. Moreover, the integrated spin densities over V(*M*) and V(C, *M*) are also close to 1.
4. For $n = 5$, the interaction in the ground state can be described in terms of two resonance structures: one with 4 unpaired electrons in C(Mn), one in V(Mn), and a pair transferred to the ligand, the other with 6 electrons in C(Mn) and one in V(Mn).
5. For $n>5$ the ground state multiplicity is $9 - n$. One electron pair can be shared by the ligand, V(*M*) and in part C(*M*). There is no spin density within V(*M*) and V(C, *M*). The charge transfer δq is close to 1 and the V(*M*) population is less than 1.
6. For Cr and Cu, the ELF function is spherically symmetrical in the core region of the metal, only one electron can be distributed over V(*M*) and V(*M*, C). The charge transfer from the metal is maximized for a bent structure.

Multicenter Bonding

Figure 11 displays the localization domains of diborane and of $Al_2C_2H_{10}$ two molecules for which a multicenter bonding is evidenced by a polysynaptic basin. In diborane, the ELF picture is consistent with *Pitzer*'s proposal [62] of a protonated

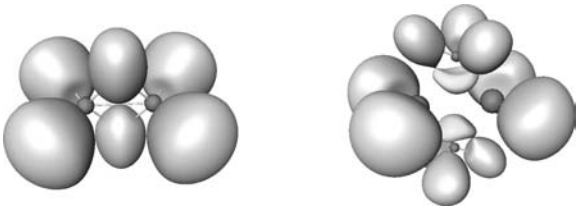

Fig. 11. $\eta(\mathbf{r}) = 0.8$ localization domains of B_2H_6 (left) and $Al_2C_2H_{10}$ (right)

double bond which is accounted for by two protonated trisynaptic basins. It has been proposed [63] to generalize the agostic interaction concept initially introduced by *Brookhart* and *Green* [64] to name an unusual interaction between a CH group and a transition metal to bonds involving protonated polysynaptic basins. This definition therefore applies not only for transition metal complexes such as $RuClCH_2CH_3(PH_3)_2$ [63] or for diborane in which there is a double agostic bond but also to the protonation of two centre bonds.

The normal coordination numbers of carbon are 2, 3, and 4 for *sp*, sp^2 and sp^3 carbons. However, in $Al_2(CH_3)_6$ the sp^3 carbons of the bridging methyl groups are pentacoordinated. The ELF localization domains of the $Al_2H_4(CH_3)_2$ model molecule represented in Fig. 11 show that the carbon of the methyl groups are pentacoordinated thanks to a V(Al, C, Al) trisynaptic basin. The existence of planar tetracoordinated carbon (ptC) has been predicted by *Hoffman et al.* [65] and observed afterward mainly by *Erker*'s group [66]. Several bonding mechanisms have been proposed on the basis of the MO theory. The ELF analysis concludes that ptCs are sp^2 carbons which form two centre bonds and one three centre bond evidenced by a trisynaptic basin. In the $ZcCl_2C_4H_2VCl_2$ model compound, the carbon atoms of the butadiyne fragment are involved in three trisynaptic V(Zr, C, C) basins.

Molina and *Dobado* [67] have recently reinvestigated the 3*c*–4*e* bond concept within the AIM and ELF frameworks. They did not find any trisynaptic basins but showed a noticeable electron delocalization between ligands in linear structures such as ClF_2^-. This electron delocalization is weaker in T-shaped molecules and negligible in bipyramidal compounds. However, as the linear structures investigated in this paper are centro symmetric anions the origin of the delocalization should be due to the symmetry of the charge distribution rather than to a bonding effect. For these reasons, we think that the 3*c*–4*e* bond concept is misleading and therefore that it is not a useful concept to describe the bonding in molecules [68].

Shared Interactions in Solids

In crystalline systems the shared interaction involves covalent and metallic solids. Figure 12 displays the localization domains of an insulator and of a conductor, the silicon and lithium crystals respectively. The bonding in silicon is characterized by well localized V(Si, Si) disynaptic basins with populations close to 2*e*. The value of ELF at the V(Si, Si) attractors is 0.959 whereas it is 0.64 at the index 1 critical point located at the boundary of two V(Si, Si) basins. In diamond, the corresponding

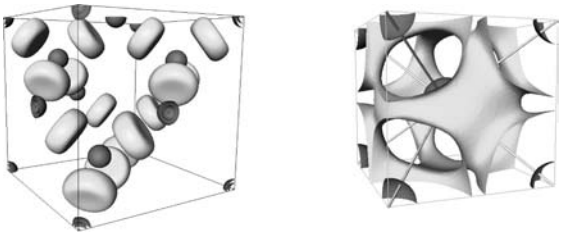

Fig. 12. Localization domains of Si (left, $\eta(\mathbf{r}) = 0.85$) and Li (right $\eta(\mathbf{r}) = 0.59$) cells

ELF values are very similar: respectively 0.944 and 0.666. Metallic bonds give rise to quite different patterns. On the one hand, the difference between the ELF values at the valence attractors and at the index 1 critical points is very small and therefore the localization domain corresponding to a value just below that of the latter critical points forms a tridimensional network. Small deviations from the jellium model, the presence of shallow maxima in the valence regions, explain this behavior [69]: these maxima remove the structural unstability of the homogeneous electron gas approximation, ELF being constant, any point is a degenerate critical point. On the other hand, the integrated density over a valence basin is always less than 2, in the case of lithium the populations of the main valence basins are close to 1, which supports the interstitial-electron model proposed by *Mo Li* and *Goddard* [70]. Moreover, metallic bonding often involves multicenter bonding evidenced by polysynaptic basins. In lithium for example, the attractors are located at the center of the faces which corresponds to a synaptic order equal to six.

Unshared Interactions

Two types of bonding mechanisms belong to the unshared interaction: the ionic bonding and bonds by delocalization such as the $3e$–$2c$ ones encountered in radical anions and cations.

Ionic Bonds

Figure 13 displays the localization domains of LiH for two internuclear distances corresponding on each side of the covalent ionic transition. As expected from chemical intuition, in the formation of an ionic bond the monosynaptic domain of the less electronegative moiety disappears because its density is transferred to the monosynaptic basin of the other subunit. In our example, the transition occurs at $R_{\mathrm{LiH}} = 2.436\,\text{Å}$.

Bonding by Delocalization

This type of bonding is characterized by large covariance matrix elements between either monosynaptic basins or even between core basins. The three electron bond in radical anions has been investigated in details by *Fourré et al*. [71]. The investigated systems are of the $\mathrm{H}_n XY\mathrm{H}_m^-$ type with $X, Y = \mathrm{Cl}$, S, P, Si, F, O, N, C and $n, m = 0$–2. The relaxed anions are characterized by the absence of a V(X, X)

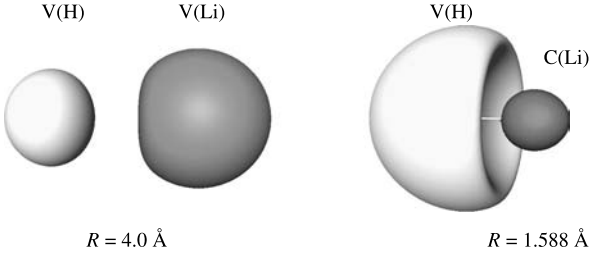

Fig. 13. $\eta(\mathbf{r}) = 0.8$ localization domains of LiH (left, $R_{\mathrm{LiH}} = 4.0\,\text{Å}$, right, $R_{\mathrm{LiH}} = 1.588\,\text{Å}$)

monosynaptic basin and by the transfer of the extra electron initially in the V(X, Y) basin of the neutral molecule into the V(X) and V(Y) monosynaptic basins. The spin density is localized within these basins and at every intermolecular separation the covariance between them is larger than 0.25, the lower bound at infinite separation.

Another interesting example of bonding by delocalization is provided by bimetallic complexes. The nature of the chemical bond in M_2(formamidinate)$_4$ complexes (M = Nb, Mo, Tc, Ru, Rh, and Pd) with different nominal bond orders ranging from 0 to 5 is a puzzling topical example which has been rationalized so far in terms of overlaps of the metal d orbitals giving rise to σ, π, and δ bonding and antibonding orbitals. In their ground state, the M_2L_4 complexes are diamagnetic and have an approximate D_{4h} symmetry. The structural properties of these second row transition metal dimer complexes can be quantitatively predicted using advanced quantum chemical methodologies [72–74].

A topological study of these systems has been recently published by *Llusar et al.* [75]. The ELF topological analysis shows a disynaptic V(M, M) basin for Ru and Rh, a group of four disynaptic V(M, M) basins for Nb and Mo, and nothing for Tc and Pd. The complexes of these two latter elements are those with the shortest (Tc) and the largest (Pd) intermetallic distances. The V(M, M) attractor multiplicity seems to be a consequence of the *Pauli* repulsion between the metallic cores which mostly depends upon the internuclear distance. Going from large to short distances there are four regimes with 0, 1, 4 and 0 attractors. The covariance matrix elements between the two C(M) basin populations accounts for about 80% of C(M) variance. The value of this index can be rationalized by simple resonance concepts. The proposed resonance structures for each metal dimer together with their weight factors calculated from the populations of the core metal basins, C(M), and their covariance values are given in Table 3. The large electron fluctuation which occurs between the two metallic cores can be interpreted in terms of simple resonance arguments, exemplified here for the Mo complex. Because the metal dimer is in a closed-shell singlet state, there is no spin polarization, and each metallic core should be considered as a local closed-shell subsystem whose orbitals fulfill the C_{4v} point group symmetry requirements. The Mo core population is close to $40e^-$ with a covariance of 1.255, and as a consequence, an average of four out of the six

Table 3. M_2(HNCHNH)$_4$; resonance structures and estimated weights

	Resonance structure	Weight
Nb	$M([\mathrm{Kr}]\pi^4)$–$M([\mathrm{Kr}]\sigma^2) \leftrightarrow M([\mathrm{Kr}]\sigma^2)$–$M([\mathrm{Kr}]\pi^4)$	1
Mo	$M([\mathrm{Kr}]\pi^4)$–$M([\mathrm{Kr}]\sigma^2\delta^2) \leftrightarrow M([\mathrm{Kr}]\sigma^2\delta^2)$–$M([\mathrm{Kr}]\pi^4)$	0.75
	$M([\mathrm{Kr}]\pi^4\delta^2)$–$M([\mathrm{Kr}]\sigma^2) \leftrightarrow M([\mathrm{Kr}]\sigma^2)$–$M([\mathrm{Kr}]\pi^4\delta^2)$	0.125
	$M([\mathrm{Kr}]\pi^4\sigma^2)$–$M([\mathrm{Kr}]\delta^2) \leftrightarrow M([\mathrm{Kr}]\delta^2)$–$M([\mathrm{Kr}]\pi^4\sigma^2)$	0.125
Tc	$M([\mathrm{Kr}]\pi^4\sigma^2)$–$M([\mathrm{Kr}]\sigma^2\delta^2) \leftrightarrow M([\mathrm{Kr}]\sigma^2\delta^2)$–$M([\mathrm{Kr}]\pi^4\sigma^2)$	1
Ru	$M([\mathrm{Kr}]\pi^4\delta^2)$–$M([\mathrm{Kr}]\pi^4\sigma^2) \leftrightarrow M([\mathrm{Kr}]\pi^4\sigma^2)$–$M([\mathrm{Kr}]\pi^4\delta^2)$	0.875
	$M([\mathrm{Kr}]\pi^4)$–$M([\mathrm{Kr}]\pi^4\sigma^2\delta^2) \leftrightarrow M([\mathrm{Kr}]\pi^4\sigma^2\delta^2)$–$M([\mathrm{Kr}]\pi^4)$	0.125
Rh	$M([\mathrm{Kr}]\pi^4)$–$M([\mathrm{Kr}]\pi^4\sigma^2\delta^2) \leftrightarrow M([\mathrm{Kr}]\pi^4\sigma^2\delta^2)$–$M([\mathrm{Kr}]\pi^4)$	0.125
	$M([\mathrm{Kr}]\pi^4\sigma^2\delta^2)$–$M([\mathrm{Kr}]\pi^4\sigma^2\delta^2)$	0.875
Pd	$M([\mathrm{Kr}]\pi^4\sigma^2\delta^2)$–$M([\mathrm{Kr}]\pi^4\sigma^2\delta^2)$	1

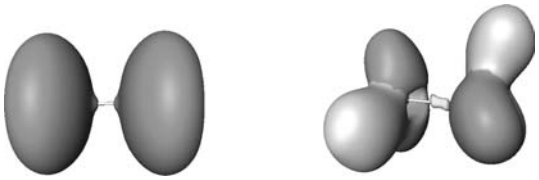

Fig. 14. Localization domains of F_2 (left, $\eta(\mathbf{r}) = 0.6$) and H_2O_2 (right, $\eta(\mathbf{r}) = 0.73$)

electrons formally considered as valence according to the MO theory should now be incorporated into the core. Following the traditional greek characters usually used to described the quadruple metal–metal bonding MOs ($\sigma^2\pi^4\delta^2$), the following core configurations are compatible with the molecular symmetry: $[Kr]\pi^4$, $[Kr]\sigma^2\delta^2$, and $[Kr]\pi^4\delta^2$ and $[Kr]\sigma^2$, $[Kr]\pi^4\sigma^2$ and $[Kr]\delta^2$. A resonance structure between the first two configurations, $Mo([Kr]\pi^4)$–$Mo([Kr]\sigma^2\delta^2) \leftrightarrow Mo([Kr]\sigma^2\delta^2)$–$Mo([Kr]\pi^4)$, corresponds to an average core population of $40e^-$ with a variance of zero.

Procovalent Bonds and Charge-shift Bonding

The study of electron density in depleted homopolar chemical bonds [76] led to introduce the concept of protocovalent bond. A protocovalent bond is characterized by two monosynaptic basins on the internuclear axis and by an ELF value at the index 1 critical point between them close to the attractor value, just like in the case of the formation or of the dissociation of a covalent bond displayed in the left part of Fig. 5. Figure 14 displays the localization domains of F_2 and H_2O_2 which are typical example of protocovalent bonding. The populations of the monosynaptic basins on the internuclear axis are very low (0.14 for F_2 and 0.29 for H_2O_2) and there are large covariance matrix elements between the monosynaptic basins of the two atoms involved in the protocovalent bond. The charge-shift bond concept introduced by *Shaik et al.* [77] in the context of the valence-bond theory explains the stabilization of this kind of bonds which is a manifestation of lone pair bond weakening. Protocovalent bonds are encountered in most homopolar *A*–*B* bonds in which both the *A* and *B* atoms have lone pairs [76, 78].

Conclusions

In this paper we have attempted to show that the ELF topological analysis provides a mathematical bridge between Quantum Mechanics and Chemistry which relies on the one hand on the statistical interpretation and on the other hand on the theory of dynamical system. This approach shares the dynamical system theory as common mathematical method with the Atoms in Molecules theory, the difference being the nature of the potential function and therefore the nature of the investigated properties. The AIM theory is rightly claimed to be rooted in Physics rather than in Chemistry and its partition scheme aims accordingly to define open quantum systems within which the virial theorem holds. Moreover, AIM does not intent to define the valence shell of an atom in a molecule and does not associate any mathematical object to bonds and lone pairs. The goal of the ELF partition is

clearly to define basins of attractors corresponding to chemical concepts, core and valence shells, bonds and lone pairs. This is achieved at the expend of the physical meaning of the basins which is lost. Another advantage of the ELF approach is that it provides pictures of the bonding in molecules which materialize the electron domains of the VSEPR model [8] and in particular to evidence the lone pairs [79]. With respect to this model, the ELF analysis had helped to refine its conclusions, in particular for the so-called hypervalent molecules [80], and to extend its applicability to the d^0 molecules of period 4 metals by considering basins of the core external shell [81].

Reactivity is another field to which the ELF approach provides useful pieces of information. For example, it enables to predict protonation sites [82] and to recover the *Holleman* rules of aromatic substitution [83–85] as well as to define aromaticity scales [86–88]. Moreover, as already mentioned, the use of catastrophe theory [44] has been applied to elucidate reaction mechanisms such as proton transfers [89–91], electron harpooning [92], isomerization [93], hydrogen intercalations [94, 95], or cycloadditions [96, 97]. Finally, it is worth noting that the graphical possibility of this approach has many possible applications for chemical education.

Mathematical Glossary

The aim of this subsection is to introduce the topological vocabulary and to provide a set of mathematical definitions.

Dynamical system. A *dynamical system* is a vector field of class C^1 bound on a manifold M. Such a vector field has no discontinuities. To any point m belonging to the M manifold corresponds one vector $X(m)$ and only one. The solutions of the system of equations $dm/dt = \mathbf{X}(m)$ are locally unique and therefore there is only one trajectory passing through m. The trajectories are determined by integrating $dm/dt = \mathbf{X}(m)$ with respect to the fictitious time variable t. The limit sets in M of $m(t)$ for $t \leftrightarrow \pm\infty$ are called the α and ω limit set.

Gradient dynamical system. The vector field of a *gradient dynamical system* is the gradient of a function called *potential function*, *i.e.*: $\mathbf{X}(m) = \nabla V(m)$.

Critical points. The *critical points* (or *limit points*) of a *dynamical system* are the points of M for which $\mathbf{X}(m_c) = 0$. A *critical point* is either an α or an ω limit of a trajectory. The set of points of M by which are built trajectories having m_c as ω limit is called the *stable manifold* of m_c, the *unstable manifold* of m_c is the set for which m_c is an α limit. The dimension of the *unstable manifold* is the *index* of the critical point. The set of the *critical points* of a *dynamical system* satisfies the *Poincaré-Hopf* formula (Eq. (15)) where I_P is the index of the *critical point P* and $\chi(M)$ the *Euler* characteristic of the manifold. A *critical point* of *index* zero is an *attractor* of the *dynamical system*. The *stable manifold* of an *attractor* is called the *basin of the attractor*. The *stable manifold* of a *critical point* of *index* greater than zero is a *separatrix*, it is the border of two or more basins. The *index* of a *critical point* m_c of a *gradient dynamical system* is the number of positive eigenvalues of the matrix of the second derivatives of the *potential function* at m_c. In this

case, a *critical point* is said to be *hyperbolic* if none of the eigenvalues is zero.

$$\sum_{P}(-1)^{I_P} = \chi(M) \tag{15}$$

Domain. If any two points a and b of a set M_A can be connected by a path belonging to M_A, the set M_A is a *domain*.

Computational Methods

The ab initio calculations of molecules have been performed at the hybrid *Hartree-Fock* density functional B3LYP level [98–101] with the *Gauss*ian 98 software [102]. The geometries have been optimized with the 6-311G(2d, 2p) basis set [103–107]. The calculations of crystalline solids have been carried out with the CRYSTAL98 software [108] and the ELF function evaluated with TOPOND98 [109]. The analysis of the ELF function has been carried out with the TopMoD program developed in the Laboratoire de Chimie Théorique de l'Université Pierre et Marie Curie [110, 111], and the ELF isosurfaces have been visualized with the Amira 3.0 software [112].

References

[1] Thom R (1972) Stabilité Structurelle et Morphogénèse. Intereditions, Paris
[2] Lewis GN (1966) Valence and the Structure of Atoms and Molecules. Dover, New York
[3] Pauling L (1948) The Nature of the Chemical Bond. Cornell University Press, Ithaca
[4] Gillespie RJ, Nyholm RS (1957) Quart Rev Chem Soc **11**: 339
[5] Gillespie RJ (1972) Molecular Geometry. Van Nostrand Reinhold, London
[6] Gillespie RJ, Hargittai I (1991) The VSEPR Model of Molecular Geometry. Allyn and Bacon, Boston
[7] Gillespie RJ (1991) Chem Soc Rev **21**: 59
[8] Gillespie RJ, Robinson EA (1996) Angew Chem Int Ed Engl **35**: 495
[9] Gillespie RJ, Popelier PLA (2001) Chemical Bonding and Molecular Geometry. Oxford University Press, Oxford
[10] Malrieu JP, Maynau D (1978) J Chim Phys **75**: 31
[11] Kutzelnigg W (2000) Theor Chem Acc **103**: 182
[12] Dirac PAM (1929) Proc Roy Soc A **123**: 714
[13] Heitler W, London F (1927) Z Physik **44**: 455
[14] Condon EU (1927) Proc Nat Acad Sci **13**: 466
[15] Pauling L (December 1954) Modern Structural Chemistry. Nobel Lecture
[16] Hoffmann R, Shaik S, Hiberty PC (2003) Acc Chem Res **36**: 750
[17] Coulson CA (1952) Valence. Clarendon, Oxford
[18] James HM, Coolidge AS (1933) J Chem Phys **1**: 825
[19] Hohenberg P, Kohn W (1964) Phys Rev **136**: B864
[20] Frisch MJ, Trucks GW, Head-Gordon M, Gill PMW, Wong MW, Foresman JB, Johnson BG, Schlegel HB, Robb MA, Replogle ES, Gomperts R, Andres JL, Raghavachari K, Binkley JS, Gonzalez C, Martin RL, Fox DJ, Defrees DJ, Baker J, Stewart JJP, Pople JA (1992) Gaussian 92, Revision B. Gaussian Inc., Pittsburgh, PA
[21] Geerlings P, De Proft F, Langenaeker W (2003) Chem Rev **103**: 1793
[22] Hammond BL Jr WAL, Reynolds PJ (1994) Monte Carlo Methods in Ab Initio Quantum Chemistry. World Scientific, Singapore, World Scientific Lecture and Course Notes in Chemistry, vol 1

[23] Daudel R (1957) Les Fondements de la Chimie Théorique. Gauthier-Villars, Paris
[24] Daudel R (1971) In: Daudel R, Pullman A (eds) Aspects de la Chimie quantique Contemporaine. Editions du Centre National de la Recherche Scientifique, Paris, p 70
[25] Aslangul C, Constanciel R, Daudel R, Kottis P (1972) In: Löwdin PO (ed) Advances in Quantum Chemistry. Academic Press, New York, vol 6, pp 93–141
[26] Daudel R (1974) Quantum Theory of The Chemical Bond. Reidel, Dordrecht
[27] Daudel R (1992) In: Encyclopedia of Physical Science and Technology. Academic Press, New York, vol 13, pp 629–640
[28] Shannon CE, Weaver W (1949) The Mathematical Theory of Communication. The University of Illinois Press, Urbana
[29] Abraham RH, Shaw CD (1992) Dynamics: The Geometry of Behavior. Addison Wesley
[30] Abraham RH, Marsden JE (1994) Foundations of Mechanics. Addison Wesley
[31] Bader RFW (1990) Atoms in Molecules: A Quantum Theory. Oxford Univ Press, Oxford
[32] Becke AD, Edgecombe KE (1990) J Chem Phys **92**: 5397
[33] Häussermann U, Wengert S, Nesper R (1994) Angew Chem Int Ed Engl **33**: 2073
[34] Silvi B, Savin A (1994) Nature **371**: 683
[35] Lewis GN (1916) J Am Chem Soc **38**: 762
[36] Diner S, Claverie P (1976) In: Chalvet O, Daudel R, Diner S, Malrieu JP (eds) Localization and Delocalization in Quantum Chemistry. Reidel, Dordrecht, vol II, pp 395–448
[37] Silvi B (2004) Phys Chem Chem Phys **6**: 256
[38] Lepetit C, Silvi B, Chauvin R (2003) J Phys Chem A **107**: 464
[39] Savin A, Becke AD, Flad J, Nesper R, Preuss H, von Schnering HG (1991) Angew Chem Int Ed Engl **30**: 409
[40] Savin A, Jepsen O, Flad J, Andersen OK, Preuss H, von Schnering HG (1992) Angew Chem Int Ed Engl **31**: 187
[41] Savin A, Nesper R, Wengert S, Fässler TF (1997) Angew Chem Int Ed Engl **36**: 1809
[42] Silvi B (2003) J Phys Chem A **107**: 3081
[43] Häussermann U, Wengert S, Nesper R (1994) Angew Chem Int Ed Engl **33**: 2069
[44] Krokidis X, Noury S, Silvi B (1997) J Phys Chem A **101**: 7277
[45] Savin A, Silvi B, Colonna F (1996) Can J Chem **74**: 1088
[46] Calatayud M, Andrés J, Beltrán A, Silvi B (2001) Theoret Chem Acc **105**: 299
[47] Cremer D, Kraka E (1984) Angew Chem Int Ed Engl **23**: 627
[48] Cremer D, Kraka E (1983) Croat Chem Acta **57**: 1259
[49] Bianchi R, Gervasio G, Marabello D (2000) Inorg Chem **39**: 2360
[50] Bader RFW, Stephens ME (1975) J Am Chem Soc **97**: 7391
[51] Cioslowski J, Mixon ST (1991) J Am Chem Soc **113**: 4142
[52] Ángyán JG, Loos M, Mayer I (1994) J Phys Chem **98**: 5244
[53] Fradera X, Austen MA, Bader RFW (1998) J Phys Chem A **103**: 304
[54] Fradera X, Poater J, Simon S, Duran M, Solá M (2002) Theor Chem Acc **108**: 214
[55] Poater J, Solá M, Duran M, Fradera X (2002) Theor Chem Acc **107**: 362
[56] Chesnut DB (2001) Chem Phys **271**: 9
[57] Fuster F, Silvi B (2000) Theoret Chem Acc **104**: 13
[58] Kutzelnigg W (1984) Angew Chem Int Ed Engl **23**: 272
[59] Grützmacher H, Fässler TF (2000) Chem Eur J **6**: 2317
[60] Chesnut DB (2002) Heteroatom Chem **13**: 53
[61] Pilmé J, Silvi B, Alikhani M (2003) J Phys Chem A **107**: 4506
[62] Pitzer KS (1946) J Am Chem Soc **67**: 1126
[63] Silvi B (2002) J Mol Struct 1659
[64] Brookhart M, Green M, Wong LL (1999) Prog Inorg Chem **36**: 1
[65] Hoffman R, Alder R, Wilcox CF Jr (1970) J Am Chem Soc **92**: 4992

[66] Erker G, Zwettler R, Krüger C, Noe R, Werner S (1990) J Am Chem Soc **112**: 9620
[67] Molina Molina J, Dobado J (2001) Theor Chem Acc **105**: 328
[68] Choukroun R, Donnadieu B, Zhao JS, Cassoux P, Lepetit C, Silvi B (2000) Organometallics **19**: 1901
[69] Silvi B, Gatti C (2000) J Phys Chem A **104**: 947
[70] Li M, Goddard III WA (1989) Phys Rev **B40**: 12155
[71] Fourré I, Silvi B, Sevin A, Chevreau H (2002) J Phys Chem A **106**: 2561
[72] Cotton FA, Feng X (1997) J Am Chem Soc **119**: 7514
[73] Cotton FA, Feng X (1998) J Am Chem Soc **120**: 3387
[74] Demachy I, Lledos A, Jean Y (1999) Inorg Chem **38**: 5443
[75] Llusar R, Beltrán A, Andrés J, Fuster F, Silvi B (2001) J Phys Chem A **105**: 9460
[76] Llusar R, Beltrán A, Andrés J, Noury S, Silvi B (1999) J Comput Chem **20**: 1517
[77] Shaik S, Maitre P, Sini G, Hiberty PC (1992) J Am Chem Soc **114**: 7861
[78] Beltrán A, Andrés J, Noury S, Silvi B (1999) J Phys Chem A **103**: 3078
[79] Chesnut DB (2000) J Phys Chem A **104**: 11644
[80] Noury S, Silvi B, Gillespie RG (2002) Inorg Chem **41**: 2164
[81] Gillespie RJ, Noury S, Pilmé J, Silvi B (2004) Inorg Chem **43**: 3248
[82] Fuster F, Silvi B (2000) Chem Phys **252**: 279
[83] Fuster F, Sevin A, Silvi B (2000) J Phys Chem A **104**: 852
[84] Fuster F, Sevin A, Silvi B (2000) J Comput Chem **21**: 509
[85] Silvi B, Fuster F, Kryachko E, Tishchenko O, Nguyen MT (2002) Molec Phys **100**: 1659
[86] Chesnut DB, Bartolotti LJ (2000) Chem Phys **253**: 1
[87] Chesnut DB, Bartolotti LJ (2000) Chem Phys **257**: 171
[88] Santos JC, Tiznado W, Contreras R, Fuentealba P (2004) J Chem Phys **120**: 1670
[89] Krokidis X, Goncalves V, Savin A, Silvi B (1998) J Phys Chem A **102**: 5065
[90] Krokidis X, Vuilleumier R, Borgis D, Silvi B (1999) Molec Phys **96**: 265
[91] Alikhani ME, Silvi B (2004) J Mol Struct **706**: 3
[92] Krokidis X, Bernard Silvi B, Sevin A (1998) New J Chem **22**: 1341
[93] Krokidis X, Silvi B, Alikhani ME (1998) Chem Phys Lett **292**: 35
[94] Michelini MC, Sicilia E, Russo N, Alikhani ME, Silvi B (2003) J Phys Chem A **107**: 4862
[95] del Carmen Michelini M, Russo N, Alikhani ME, Silvi B (2004) J Comp Chem **25**: 1647
[96] Berski S, Andrés J, Silvi B, Domingo L (2003) J Phys Chem A **107**: 6014
[97] Polo V, Andres J, Castillo R, Berski S, Silvi B (2004) Chem Eur J (in press)
[98] Becke AD (1993) J Chem Phys **98**: 5648
[99] Becke AD (1988) Phys Rev **A38**: 3098
[100] Lee C, Yang Y, Parr RG (1988) Phys Rev **B37**: 785
[101] Miechlich B, Savin A, Stoll H, Preuss H (1989) Chem Phys Lett **157**: 200
[102] Frisch MJ *et al*. (1998) Gaussian 98, Revision A.9. Gaussian Inc, Pittsburgh, PA
[103] Wachters AJH (1970) J Chem Phys **52**: 1033
[104] Clark T, Chandrasekhar J, Spitznagel GW, von Ragué Schleyer P (1983) J Comput Chem **4**: 294
[105] Frisch MJ, Pople JA, Binkley JS (1984) J Chem Phys **80**: 3265
[106] MacLean AD, Chandler GS (1980) J Chem Phys **72**: 5639
[107] Krishnan R, Binkley JS, Seeger R, Pople JA (1980) J Chem Phys **72**: 650
[108] Saunders VR, Dovesi R, Roetti C, Causà M, Harrison NM, Orlando R, Zicovitch-Wilson CM (1998) CRYSTAL98, User's manual
[109] Gatti C (1998) Topond98 manual
[110] Noury S, Krokidis X, Fuster F, Silvi B (1997) Topmod package
[111] Noury S, Krokidis X, Fuster F, Silvi B (1999) Comput in Chem **23**: 597
[112] Template Graphics Software (2002) Amira 3.0. TGS Inc., San Diego, CA